

Modelling and Control of a Grid-connected Hybrid photovoltaic/wind/battery System Coupled to an AC Load

Mohamed Yassine Allani^{1†}, Fernando Tadeo^{2†}, Dhafer Mezghanni^{3†} and Abdelkader Mami^{4†}

Faculty of Sciences of Tunis, Tunis-El Manar University, 2092 El-Manar-Tunis, Tunisia

Summary

This paper describes the development and the optimization of a novel hybrid system (composed of photovoltaic panel, wind energy, converters and batteries), connected to the grid. To acquire the maximum power, two MPPT commands based on fuzzy logic are used. In addition, the control of the battery focuses on regulating the DC voltage. A high voltage gain DC-DC converter makes possible to increase the voltage supplied by the DC bus (24V) to a sufficient voltage for the inverter (aprox. 400V) and minimize power losses to ensure the maximum total efficiency of the chain. The use of single phase inverter controlled by VOC and a LCL filter allows to connect this hybrid system to the AC loads and the grid. For validation purposes, the system is modelled and simulated using MATLAB/SIMULINK. Results shows that the system can appropriately work in the climatic conditions variation like the wind speed and the radiation.

Key words:

Hybrid systems, renewable energies, batteries, single phase inverter, buck converter, high-gain dc-dc converter, bidirectional converter, fuzzy logic controller.

1. Introduction

Today, much of world's energy production is provided by fossil sources, generating greenhouse gas emissions and pollution. The exploitation of renewable energies is necessary to reduce this dependency. This paper concentrates on distributed hybrid sources: A hybrid system of energy provided locally by wind turbines generators (WTG), photovoltaic generators (PVGs), assisted by batteries in a grid-connected configuration [1], as an alternative to standalone applications [2]. For this, power converters and control units are needed for power management, making possible to provide power reliably, extracting the maximum power delivered by PVG and WTG. Hybrid system architectures have been already studied in the literature: for example in [3] PVG, a WTG, converters, a storage source and DC loads were considered. The behavior of the Constant Power Load during the failure was evaluated, with these renewable power generators supplying according to their characteristics. In addition, these converters have a limiting stage that restricts the fault current of this resource. As a result of the low power of PVG and WTG in this hybrid system, the majority of the fault is injected from the power grid. The most important

contribution to the fault current injected by all resources is caused by the grid.

For this purpose, there are several methods of PPM prosecution in the literature such as increment and conductance [4], method of parasitic capacitance [5] or method of perturb and observe [6], etc. They are based on the adjustment of the current or the voltage of the renewable source according to the variation of the climatic conditions and/or of exploitations. However, uncertainties about these conditions decreased the efficiency of these methods, especially under the variations of the solar radiation, wind speed and temperature.

Artificial intelligence methods like neural networks [7] and fuzzy logic [8, 9] have the qualities of adaptive and flexible mechanisms, which are able to improve the efficiency of the control system in the presence of these uncertainties. Fuzzy logic control is used frequently to extract the maximum power delivered by PVG [8-11], and WTG [12], as it makes possible to easily implement power management rules. Moreover, it can work with inaccurate inputs, and does not require a perfectly known mathematical model. In addition, it is robust and adaptive providing good performance in the presence of variation of the system parameters and disturbances.

Besides, to increase the voltage of the micro-grid used in the grid connection starting from 24V until 400V, conventional boost or buck/boost choppers are the first choice for anyone trying to achieve higher output voltages than the input [13]. Its converters require higher duty cycles to reach higher voltages, which implies large input currents. They would increase conduction losses in the MOSFET or switching IGBT. As a result, the efficiency of the converter is reduced. The peak blocking voltage of the transistor is equal to the output voltage. In addition, due to a high output voltage and high pulse currents, there is a serious reverse recovery problem in the diode of both converters. In summary, the parasitic losses, the high voltage on the switch and the serious problem of reverse diode recovery make both converters unusable for use as high voltage gain converters. The second obvious choice would be conventional isolated converters [14-16] such as forward, fly-back, half-bridge, full-bridge and push-pull converters. The voltage gain of these converters depends on the transformer transformation ratio or the coupled inductances. Therefore, these converters can achieve high voltage gains

by using a higher transformer ratio on their transformers or coupled inductors. However, these converters consume a discontinuous input current, making them unsuitable for renewable energy applications such as photovoltaic panels and wind turbines. They would need large input filter capacitors to be able to operate with renewable sources. In addition, the leakage inductance in these converters leads to an increase in the voltage peaks on its switches. Consequently, the clamping circuits required to protect the switches complicate the system design. As conventional uninsulated and isolated converters failed in one way or another, new high voltage gain DC-DC converters were found. The integration of this high gain dc-dc converter into renewable energy systems has not been treated in the literature, but the conventional converters previously presented have been the subject of several studies [17], [18]. This contribution is presented as an original work given the application of a robust fuzzy logic type control applied to this high gain DC-DC converter in order to guarantee robust performance with regard to variations in climatic conditions (temperature, solar radiation, wind speed) and takes into consideration the hybridization of energy sources (PV, wind, battery). For this reason, it is possible to use one of high-voltage-gain dc-dc family converters as the favored alternative [19].

A number of different methods of current control have already been proposed to regulate power exchange with the single-phase grid while reducing harmonic distortions in alternating current, such as hysteresis current control [20], [21], voltage orientation control [22], [23] and resonance-based proportional control (PR) [24], [25], all of which have their own advantages and disadvantages. Therefore, the voltage orientation control was dedicated to the control of the single-phase inverter.

The paper is structured as follows: Section II presents the modelling of the global hybrid system; the strategies of the control applied are illustrated in Section III. Some simulation results are provided and discussed in Section 4. The conclusion appears at the end of this work.

Nomenclature:

- PVG Photovoltaic Generator
- WTG Wind Turbine Generator
- MPPT Maximum Power Point Tracking
- VOC Voltage Oriented Control

- I The output current of the PVG
- I_{ph} The photocurrent of the solar Panel
- I_d The diode current of the solar Panel
- I_o The photovoltaic reserve saturation current diode
- a The ideality factor
- k The Botzman Constant
- k_T The temperature coefficient in current
- T The temperature

- T_{ref} The reference Temperature
- q The elementary charge in Coulomb
- G The irradiance
- G_{ref} The reference irradiance
- E_{gap} The Gap energy.

2. Modelling of global hybrid system

Different architectures of hybrid power systems have been developed in literature: see for example, [13], [26]-[30]. The hybrid system considered here is composed of a photovoltaic generator, a wind turbine generator, a battery bank (24V), an uncontrolled rectifier, a single phase inverter, a filter, two buck converters, a high gain boost converter and a bidirectional buck-boost converter connected to the grid with an AC load. Fig. 1 shows the global hybrid system proposed.

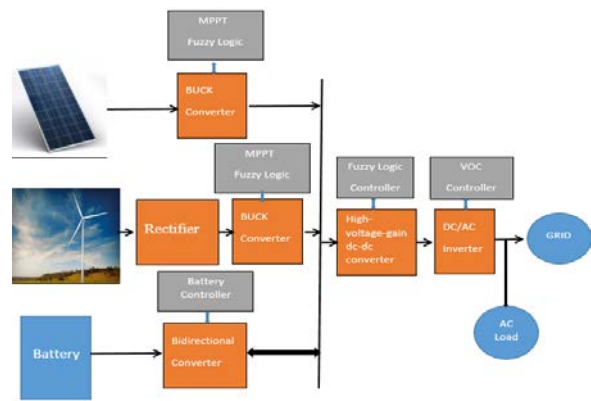


Fig. 1 Hybrid local power system

2.1 Modelling of the photovoltaic source (PVG)

A photovoltaic panel consists of several modules connected in series and in parallel to obtain desired voltages and power. Every module is collected of numerous PV cells in parallel and in series. A comparison made in [27] between the two-diode model and the one-diode model under the same conditions, shows that the series resistance marks the difference between the different models and that the one-diode model combines simplicity, precision and presents the choice that is considered most interesting. Fig. 2 displays the electrical model of the PV cell, described by the current I_{ph} , depending on the photovoltaic irradiation in parallel with a diode and the shunt resistor R_{sh} , the entire components are mounted in series with the resistance R_s . A photovoltaic cell is then represented by the following equations [9], [13]:

$$I = I_L - I_d \quad (1)$$

$$I_d = I_o \cdot [\exp(\frac{q \cdot V_{pv}}{akT}) - 1] \quad (2)$$

$$I_L = [I_{sc} + k_I \cdot (T - T_{ref})] \frac{G}{G_{ref}} \quad (3)$$

$$I_o = I_{os} \left(\frac{T}{T_{ref}}\right)^{\frac{3}{a}} \cdot \exp\left[\frac{q \cdot E_{gap}}{akT} \left(\frac{1}{T_{ref}} - \frac{1}{T}\right)\right] \quad (4)$$

$$I_{os} = \frac{I_{sc}}{\exp(\frac{q \cdot V_{oc}}{akT_{ref}}) - 1} \quad (5)$$

$$I = I_L - I_o \cdot [\exp(\frac{q \cdot (V_{pv} + I_{pv} \cdot R_s)}{akT}) - 1] - \left(\frac{V_{pv} + I_{pv} \cdot R_s}{R_{sh}}\right) \quad (6)$$

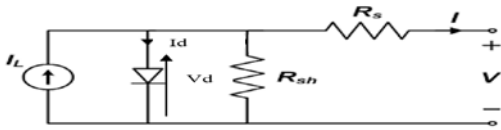


Fig. 2 Electric model used for the photovoltaic cell

For example, some parameters for the PV model used for validation are presented in Table 1.

Table 1: Kaneka G-SA060 values used with MATLAB/Simulink (at standard test conditions: 1000W/m² & 25°C) [9], [13], [26]

Parameters of PV	Values and units
Pmax(W)	60.3 W
Cells per Module	61
Vpv at Pmax(V)	67 V
Ipv at Pmax(A)	0.9 A
Vo(Open Circuit Voltage)(V)	91.8 V
Is(Short Circuit Current)(A)	1.19 A
a	2.1922
Rs(Series Resistance)(ohm)	5.8 ohms
Rsh(Shunt Resistance)(ohm)	254.8 ohms

2.2 Modelling of the Wind Source (WTG)

The wind turbine generator is regularly constructed by a stable magnetic synchronous generator. In this work, three uncontrolled phase rectifiers are assumed, composed of six diodes that implement the AC/DC electric conversion. The characteristic parameters of the wind turbine generator are presented in Table 2.

Table 2: The Wind Turbine Generate parameters used in the simulation (AIR X Wind Turbine) [13]

Parameter	Value
Rotor Diameter	46 in (1.15 m)
Weight	13 lb (5.85 kg)
Start Up Wind Speed	15.6 mph (7.5 m/s)
Voltage	24 VDC
Rated Power	386 watts at 28 mph (12.5 m/s)
Base rotational speed	1700 rpm
Initial rotational speed	500 rpm
Moment of inertia	kg.m ²

➤ Modelling of wind turbine:

The power provided by the wind turbine can be estimated by:

$$P_{turb} = \frac{1}{2} C_p(\beta, \lambda) \rho \pi R^2 V_w^3 \quad (7)$$

Where R is the radius of the wind turbine, $\beta = 0$ is the pitch angle, C_p is the power coefficient, V_w the wind speed, and λ symbolize the tip speed ratio defined by:

$$\lambda = \frac{R \omega_{turb}}{V_w} \quad (8)$$

Where ω_{turb} characterizes the angular velocity of the rotor of the wind turbine.

➤ Modelling of PMSG:

Several types of the wind turbine generator was proposed used recently, the most popular one is the PMSG generator which is especially used for small ones. The following calculations describes the mathematical model of the PMSG [12]:

$$V_q = R_s i_q - L_q \frac{di_q}{dt} + w_e L_d i_d + w_e \lambda_m \quad (9)$$

$$V_d = R_s i_d - L_d \frac{di_d}{dt} + w_e L_q i_q \quad (10)$$

The electromagnetic torque is expressed by:

$$T_{em} = \left(\frac{3P}{2}\right) [(L_d - L_q)] i_q i_d - i_q \lambda_m \quad (11)$$

The electrical angular speed ω_e depends on the number of poles pairs P , although the mechanical angular speed ω_{turb} is given by equation (12).

$$w_e = \frac{P}{2} w_{turb} \quad (12)$$

➤ The three phase uncontrolled modelling of the rectifier:

➤ The rectifier transforms AC to DC. There are two main types of rectifier: controlled and uncontrolled. In this case, the PMSG electrical model is presented in Fig.3 where it is connected to the three phase uncontrolled rectifier composed with six diode. The relations bellow characterize the expression of PMSG which is the prompt voltage V , V_{DC} which is the DC output voltage and the current I_{DC} :

$$V = V_m \sin(\omega t) \quad (13)$$

$$V_{dc} = \frac{3\sqrt{3}}{\pi} V_m = \frac{3\sqrt{6}}{\pi} \lambda P w_e \quad (14)$$

$$I_{DC} = \frac{\pi}{\sqrt{6}} I_A \quad (15)$$

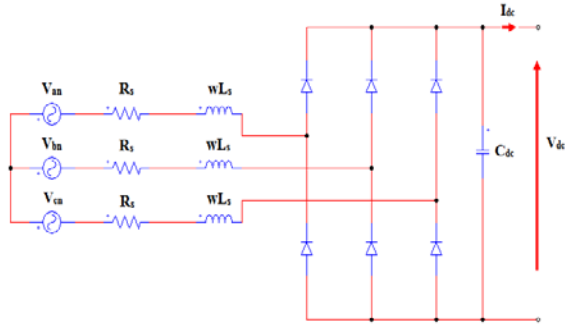


Fig. 3 Equivalent circuit of PMSG with rectifier [26]

2.3 The Buck Converter modeling

The buck converter is chosen to allow the reduction of the voltage distributed by the PVG and the WTG. Thus, the maximum power delivered by each sources should be extracted [13]. The electrical model of the buck converter is illustrated in Fig. 4 where the current and the DC output voltage are presented by the expression (16).

$$\begin{cases} V_{out} = \alpha_{buck} V_{in} \\ I_{out} = \left(\frac{1}{\alpha_{buck}}\right) I_{in} \end{cases} \text{ with } 0 < \alpha_{buck} < 1 \quad (16)$$

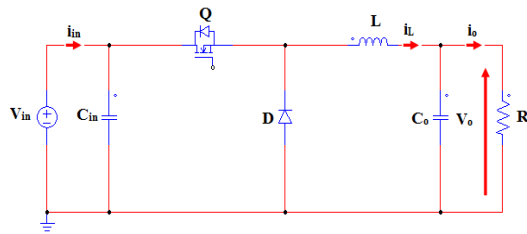


Fig. 4 The electrical circuit of the buck converter [28]

The parameters presented in Table 3 and Table 4 are obtained from the PV and the WTG sources of the buck converter, respectively.

Table 3: Design of the buck converter for the PV generator system

Parameters	Values
Input Voltage	61 V
Output Voltage	24 V
Duty Cycle	0.3998
Inductance	10 μ H
Input Capacitor	470 μ F
Output Capacitor	470 μ F
Cutting Frequency	30 kHz

Table 4: Design of the buck converter for the WT generator system

Parameters	Values
Input Voltage	160 V
Output Voltage	24 V
Duty Cycle	0.15
Inductance	20 μ H
Input Capacitor	470 μ F
Output Capacitor	470 μ F
Cutting Frequency	30 kHz

2.4 Modelling of the High-Voltage-Gain DC-DC Converter

The renewable energy integration and the energy storage need a 400 V DC to connect to the grid. Therefore, a boost converter or a buck-boost converter used to increase the voltage to 24V to 400V DC would involve a great ratios of duty, that fallouts a higher stress devices and lower efficiency. Hence, it is possible to use one of high-voltage-gain dc-dc family converters as a preferred choice [19]. Consequently, the electrical circuit of the high -voltage-gain dc-dc converter is shown in Figure 5. For this type of converter, the input power is transmitted to the output by the charge/discharge of the capacitors of the voltage booster circuit, powered by two input sources. Thus, switches S1 and S2 each have their own duty cycle. The voltages of the circuit capacitors and the output voltage are simplified as indicated in the relationships (17), (18), (19), (20) and (21), respectively [19].

$$\langle V_{L1} \rangle = \langle V_{L2} \rangle = 0 \quad (17)$$

$$V_{Ax} = V_{C2} + V_{C3} = V_{out} - V_{C1} - V_{C4} = \frac{V_{e1}}{(1-\alpha_1)} \quad (18)$$

$$V_{Bx} = V_{C1} + V_{C2} = V_{out} - V_{C4} - V_{C3} = \frac{V_{e2}}{(1-\alpha_2)} \quad (19)$$

$$V_{C2} = V_{C3} = \frac{1}{2} * \frac{V_{e1}}{(1-\alpha_1)} \quad (20)$$

$$V_{C1} = V_{C4} = \frac{1}{2} * \frac{V_{e1}}{(1-\alpha_1)} + \frac{V_{e2}}{(1-\alpha_2)} \quad (21)$$

The proposed converter is powered by a single input source. For this reason, the switches S1 and S2 have the same duty cycle and are shifted 180 degrees from each other. The voltages of the circuit capacitors and the output voltage are simplified as illustrated in equations (22), (23) and (24), respectively.

$$V_{out} = \frac{2V_{e1}}{(1-\alpha_1)} + \frac{2V_{e2}}{(1-\alpha_2)} \quad (22)$$

$$V_{C2} = V_{C3} = \frac{1}{2} * \frac{V_e}{(1-\alpha)} \quad (23)$$

$$V_{C1} = V_{C4} = \frac{3}{2} * \frac{V_e}{(1-\alpha)} \quad (24)$$

The relations that express the output voltage and the inductances of the selected converter are given in equations (25) and (26), respectively.

$$V_{out} = \frac{4.V_e}{(1-\alpha)} \text{ with } 0.5 < \alpha < 0.9 \quad (25)$$

The expression for the inductances can be described as:

$$L_1 = L_2 = L = \frac{\alpha.V_{in}}{\Delta I_L - f_{sw}} \quad (26)$$

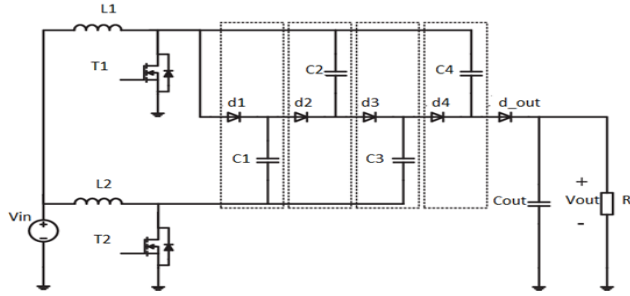


Fig. 5 The electric circuit of the high –voltage-gain dc-dc converter [18]

2.5 Modelling of the single phase inverter

Different types of inverter can be used to integrate the renewable energy to the grid [32]. In our work, the single phase inverter was composed by four IGBT, which makes the DC/AC electric conversion. The electrical model of the inverter is displayed in Fig. 6.

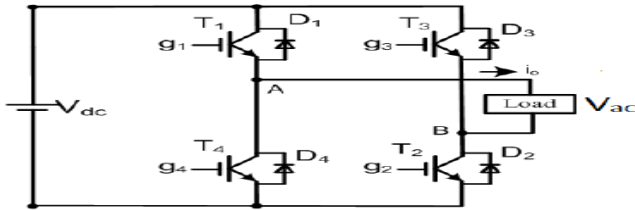


Fig. 6 The electric circuit of the single phase inverter [32].

2.6 Modelling of the LCL filter

Generally, there are four different types of filters; L filter, LC filter, LCL filter and LLCL filter [20]. It is preferred to choose in this work the LCL filter, which provides a high attenuation beyond the resonance frequency and give a better decoupling capability between the filter and the grid impedance. The electrical model is presented in Fig. 7.

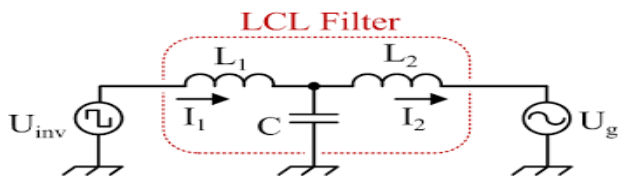


Fig. 7 LCL filter design [20]

2.7 Modelling of the Battery (Lithium-Ion)

Several types of batteries are used in this kind of hybrid systems [34]. Table 5 recapitulate the technical parameters of the lithium-Ion battery used in this work.

Table 5: Parameters of the battery used in the simulation (lithium-Ion) [34]:

Parameters	Values
Nominal Voltage	24 V
Maximum Capacity	100 Ah
Cut-off Voltage	18 V
Fully Charged Voltage	27.9 V

3. Control strategies of the hybrid system:

3.1 The Maximum Power Point Tracking (MPPT) of the PVG and WTG:

Recently, different approaches used to control the maximum power supplied by renewable energy sources have been presented in the literature. The conductance and incremental method is frequently applied in photovoltaic and wind power systems [4], [34], [35]. It tracks the MPP by comparing the instantaneous and incremental conductance of the source under examination. The question of the conductance and incremental method is similar to that of perturbation and observation. A fixed step size is usually adopted, which specifies the accuracy and speed of the MPPT response. In this technique, the term $\frac{dI}{dV}$ is compared to $-\frac{I}{V}$. The maximum power point is achieved when this difference is zero.

$$\frac{dP}{dV} = I \frac{dV}{dV} + V \frac{dI}{dV} = I + V \frac{dI}{dV} = 0 \tag{27}$$

$$-\frac{I}{V} = \frac{dI}{dV} \tag{28}$$

dV and dI can be expressed by:

$$dV(k) \approx \Delta V(k-1) = V(k) - V(k-1) \tag{29}$$

$$dI(k) \approx \Delta I(k-1) = I(k) - I(k-1) \tag{30}$$

As a result, to examine the running of one of the renewable energy sources (photovoltaic or wind) and the power at load, the following inequalities are proved:

$$\frac{dP}{dV} > 0 \text{ for } V < V_{mp} \tag{31}$$

$$\frac{dP}{dV} = 0 \text{ for } V = V_{mp} \tag{32}$$

$$\frac{dP}{dV} < 0 \text{ for } V > V_{mp} \tag{33}$$

Therefore, the proposed control combines the incremental and conductance method and fuzzy logic in a fuzzy controller, taking into account the direction of the variation of the disturbances. Based on the previous equations of the incremental and conductance technique, we have:

$$\frac{d(V * I)}{dV} = I + V \frac{dI}{dV} = 0 \tag{34}$$

$$-\frac{I}{V} = \frac{dI}{dV} \tag{35}$$

This equality shows that the renewable energy source (photovoltaic or wind) is at its maximum power value. This equality is used to design our fuzzy controller whose inputs are:

$$E(k) = \frac{I}{V} + \frac{dI}{dV} \tag{36}$$

$$dE(k) = E(k) - E(k - 1) \tag{37}$$

The Fuzzy logic control based on the incremental and the conductance is one of the most known techniques of the MPPT [8]. It makes possible to consider current and voltage, to calculate the command that maximizes the use of local power sources. The fuzzy logic controller model simulated under MATLAB/SIMULINK software is presented in Fig. 7.

Triangular membership functions for the fuzzification and defuzzification process are used. For the two inputs and the output of each source, 5 belonging functions have been identified according to the following linguistic variables: Large negative (GN), negative (N), zero (Z), positive (P) and large positive (GP). Fig. 8 and Fig. 9 describes the degree of membership function obtained on the input and the output of the PV and the WTG, respectively.

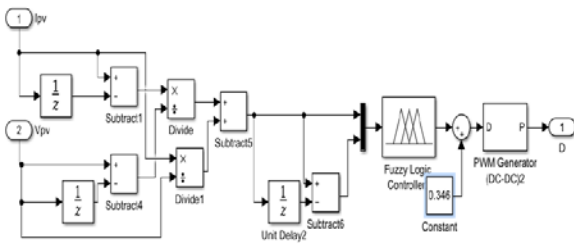


Fig. 7 Simulink model of the fuzzy logic controller

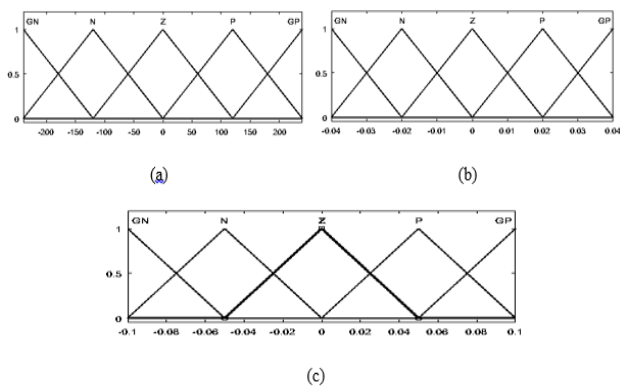


Fig. 8 The membership function of input and output of PV: (a) dE, (b) E and (c) Duty cycle.

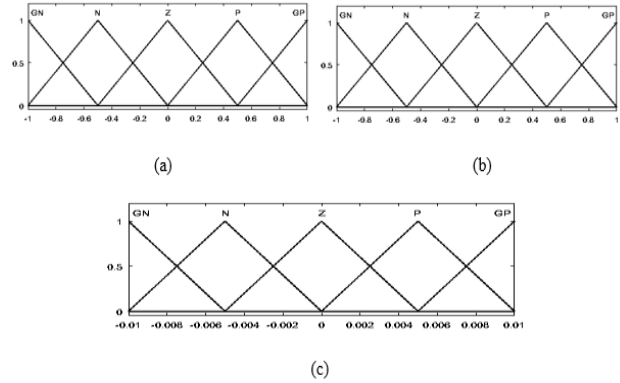


Fig. 9 The membership function of input and output of WTG: (a) dE, (b) E and (c) Duty cycle.

3.2 Charge and Discharge Controller for the Battery

The procedure used on the control of the battery consist on charging and discharging the battery until maintaining a constant value of the DC bus. The model of the battery controller is illustrated in Fig. 10.

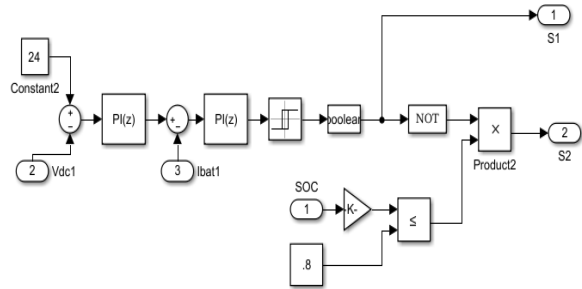


Fig. 10 Control of the battery using the charge and discharge strategy

The value of parameters PI is illustrated in table 7.

	Ki	Kp
Voltage	5	0.01
Current	0.8	0.2

3.3 The Strategy Control of the High-Voltage-Gain DC-DC Converter

The control of this converter in literature is mainly based on PI controller [18], but, in this work this converter was controlled based fuzzy logic. For inputs and outputs, seven membership functions have been defined for the fuzzification and defuzzification process based on the following linguistic variables: Grand negative (GN), negative (N), negative small (NS), zero (Z), positive small (PS), positive (P) and grand positive (GP). Fig. 11 presents the membership function degree of the different inputs and outputs.

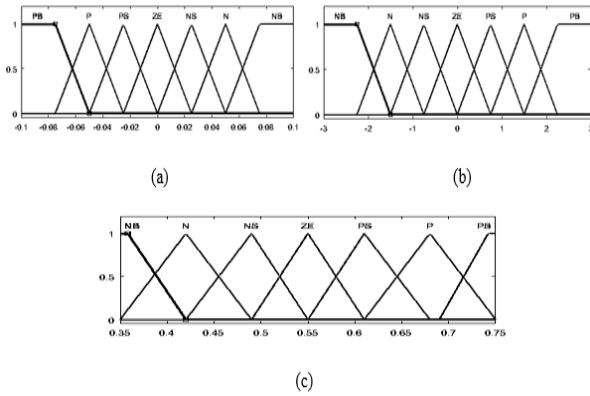


Fig. 11 The membership function of the input and output of the high-gain dc-dc converter: (a) dE, (b) E and (c) Duty cycle.

3.4 The Single Phase Inverter Strategy of Control

To regulate the power exchange with the single-phase grid while reducing harmonic distortions in the alternating current, the voltage orientation control was used to control our inverter. Fig. 12 describes the VOC control diagram.

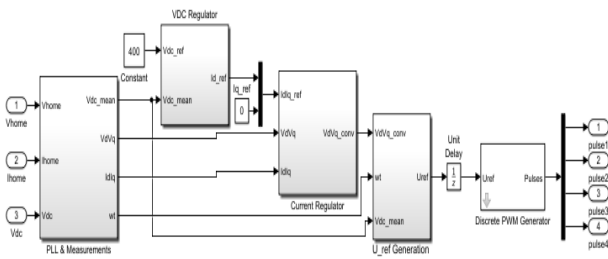


Fig. 12 The diagram of the VOC controller

The parameters value of the PI used to vary the voltage and the current inserted to the grid are demonstrated on Table 8.

Table 7: Different values of parameter PI

	Ki	Kp
Voltage	200	12
Current	6.6	0.15
PLL	3200	180

4. Simulation results and discussion

In order to justify the suggested strategies of the hybrid power system and demonstrate its efficiency, the software MATLAB/SIMULINK was used for the simulation. The global system contains the PVG composed by four PV module connected in parallel, WTG (400W). All the sources are associated to the buck converter and the battery with the bidirectional converter. This hybrid system is

related to the high-gain dc-dc converter attached to the inverter, the filter, the AC load and finally the grid

4.1 Simulation results of the PVG

The photovoltaic generator is associated to the buck converter, controlled by MPPT based on fuzzy logic controller. During the simulation, the photovoltaic radiation varied between $700W/m^2$ and $1000W/m^2$, with a temperature of $25^\circ C$. The role of the buck converter consist on the decreasing of the voltage to 24V and the extraction of the maximum power delivered by the PVG during the variation of the photovoltaic radiation. The command of fuzzy logic based on the incremental and conductance works very well and assure the PPM tracking with all variation of climatic conditions. It also operates with a good precision and rapidity. Fig. 13 presents the profile of the radiation, the power and the duty cycle obtained from the PVG.

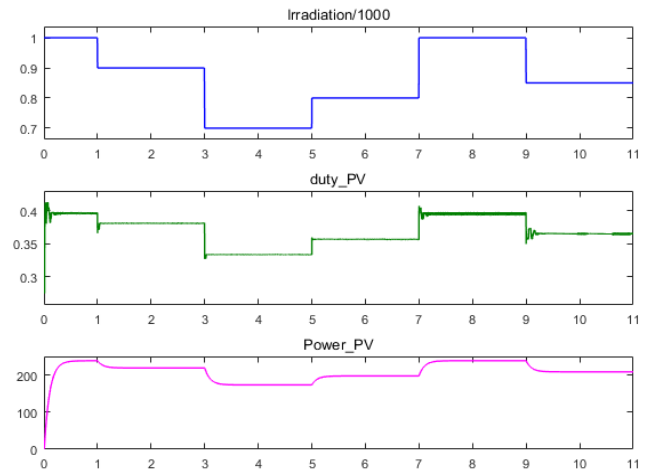


Fig. 13 The variation of the duty cycle, the power and the radiation of the PV

4.2 Simulation results of WTG

The WTG (wind turbine generator) is composed by the wind turbine and the PMSG allied to the uncontrolled rectifier, associated to the buck converter and controlled by the fuzzy logic controller, based on incremental and conductance. The role of the buck converter is to decrease the voltage to the desire value 24V and ensure that the WTG to provide the maximum power Fig. 14 shows the proportional variation between the wind speed (which is artificially changed in steps, to show the adaptability to quick wind fluctuations), the duty cycle required at the power converter, and the output power of the WTG. Therefore, the MPPT makes possible to extract the maximum power without big variations in the power, despite the important deviations of the wind speed.

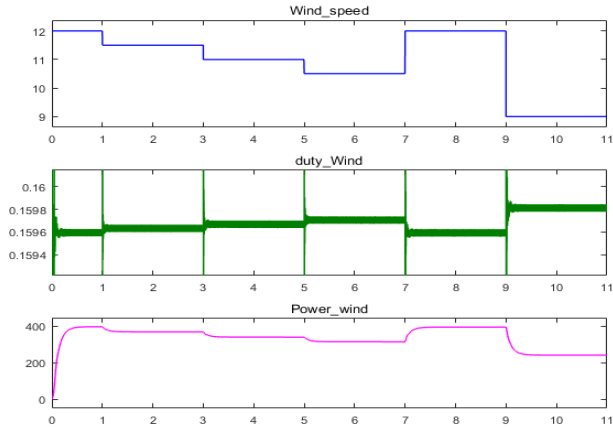


Fig. 14 Variations of wind speed, duty cycle and output power to show robustness to quick wind variations

4.3 Simulation results of the hybrid power system

Fig. 15 shows the simulation results of the output powers that are delivered by PVG, WTG and battery, and the result (power injected in the Bus DC). It can be seen that the charge and discharge of the battery is correctly regulated, utilizing the difference between the power provided by the renewable sources and the power injected in the Bus DC.

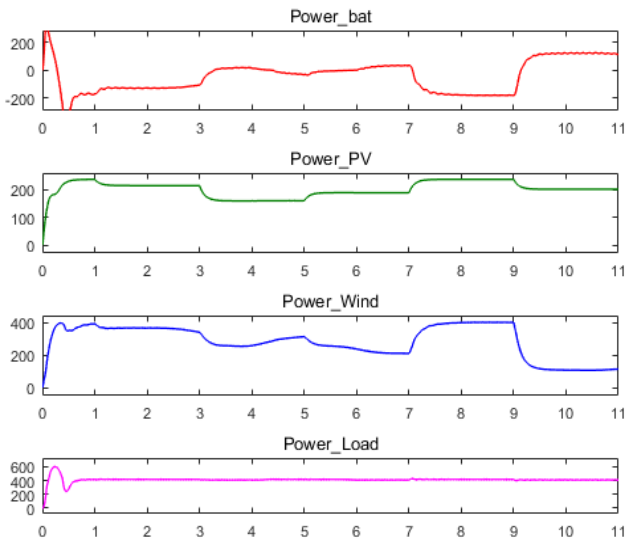


Fig. 15 Simulated output powers delivered by the battery, the PVG, the WTG and the Bus DC

The battery is controlled to maintain a constant voltage of the DC bus. It can be observed that the voltage value is correctly regulated between 22V and 24V, despite the significant variations of wind speed that are simulated. The results of the output power, the current and the voltage of the DC Bus are presented in Fig. 16.

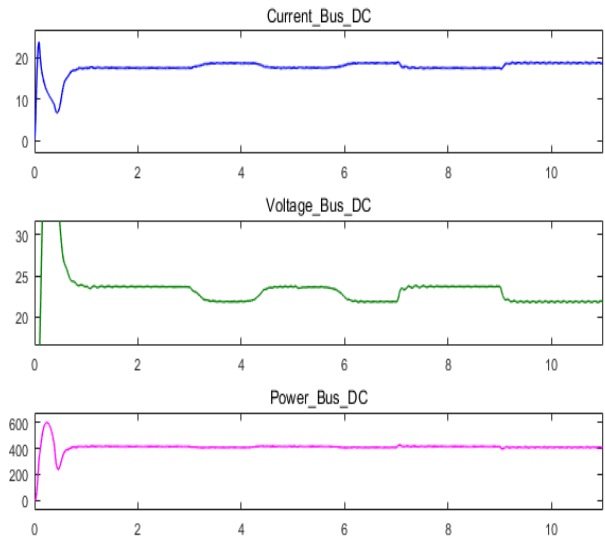


Fig. 16 The output power, current and voltage of the Bus DC.

In order to establish the connection of the hybrid system to the grid, a current of 400 V should be delivered in the input of the inverter. To achieve this, a high-voltage-gain dc-dc converter is used which allows to improve the voltage from 24V to 400V. Fig. 17 illustrates the output voltage, the current and the power of the converter profiles.

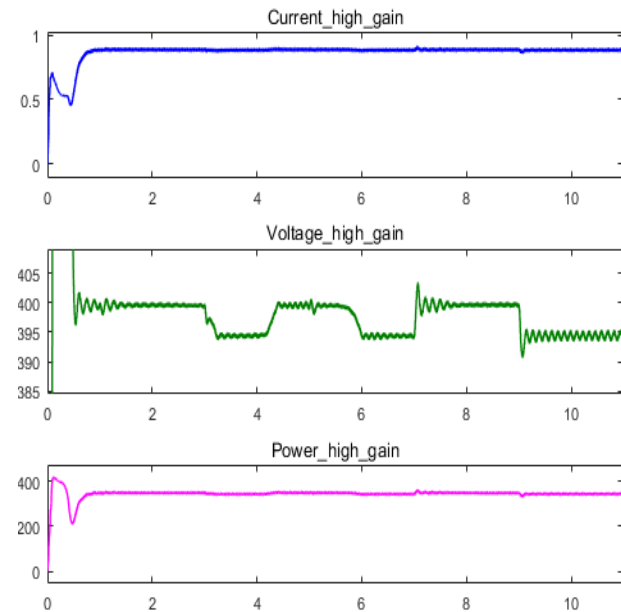


Fig. 17 Profiles of the outputs voltage, the current and the power of the high-voltage-gain dc-dc converter.

The required value of the output voltage of the converter is obtained with small current ripples. It is pointed out that the voltage value is well regulated at the preferred value of

400V. Fig. 18 presents the obtained results of the duty cycle variation of the high-gain dc-dc converter.

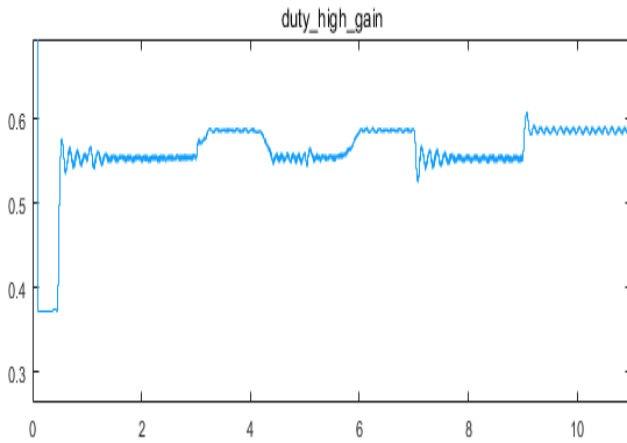


Fig. 18 Variation of the duty cycle of the high-voltage-gain dc-dc converter.

Fig. 19 shows the results of the alternative voltage and the current injected to the grid and required by the AC load.

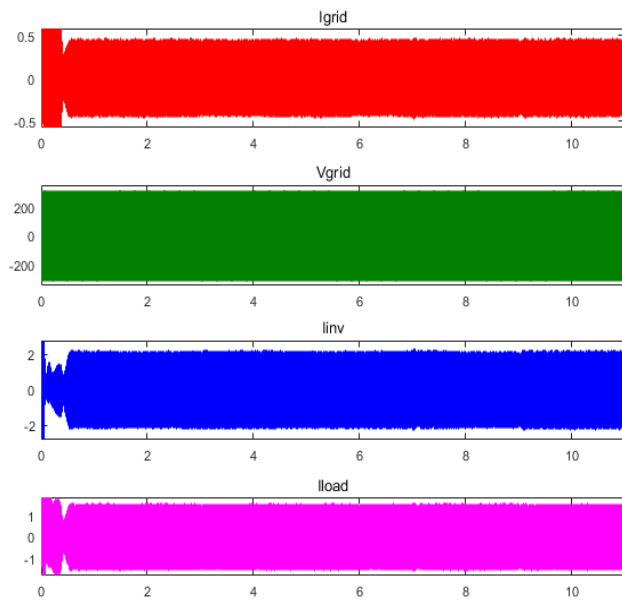


Fig. 19 The profile of I_{grid} , V_{grid} , I_{inv} and I_{load} .

Results shows that the sum of the current desired by the AC load and the current injected to the grid is efficiently equal to the current provided by the system of the hybrid power. The synchronization of the voltage and the current injected to the grid are presented with details in Fig. 20.

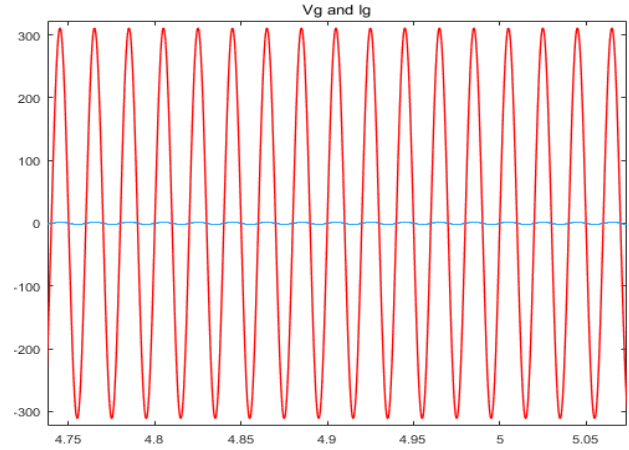


Fig. 20 The Voltage and the current injected to the grid.

5. Conclusion and Perspectives

The modeling and the control of a hybrid power system connected to the grid, to power an AC load have been developed in this paper. A control strategy based MPPT fuzzy logic control using the (incremental and conductance) algorithm is used to extract the maximum power obtained from the PVG and the WTG sources. Besides, a fuzzy logic control that provide constant DC-link voltage in the output of the high-gain dc-dc converter was presented. To control the single phase inverter an VOC is included. To charge and discharge the battery two PI controllers are proposed: the first one to regulate the voltage of the Bus DC, and the second one to regulate the current. The integration of a high voltage gain DC-DC converter makes possible to increase the 24V voltage supplied by the DC bus to a voltage appropriate for the inverter of about 400V and reduce power losses to ensure maximum efficiency of the hybrid system. In addition, the novel design presented in this work reduces the requirements on the sources used.

A comparison of the results obtained with the proposed approach and those presented in [3] is presented: it is noted that the voltage drop of the proposed system is lower similar, with a similar generated current. With the proposed models, the accuracy of studies on the hybrid power system will improve, in particular in the effect of variations of the climatic parameters, as well as the characteristics of different converters in the system.

As work perspective, a method for integration of the bidirectional inverter used for charging of the battery from the grid when there is lack of energy will be studied.

Acknowledgments

The authors would like to express their cordial thanks to Pr. Abdelkader Mami for his valuable advice.

References

- [1] Dorin Petreus, Stefan Daraban, Marcian Cirstea "Modular Hybrid Energy Concept Employing a Novel Control Structure Based on a Simple Analog System," *Advances in Electrical and Computer Engineering*, vol. 16, no.2, pp.3 – 10, 2016
- [2] Bayati, Navid, Amin Hajizadeh, and Mohsen Soltani. "Accurate Modeling of DC Microgrid for Fault and Protection Studies." 2018 International Conference on Smart Energy Systems and Technologies (SEST). IEEE, 2018.
- [3] Limunita Barote, Corneliu Marinescu "Modeling and Operational Testing of an Isolated Variable Speed PMSG Wind Turbine with Battery Energy Storage," *Advances in Electrical and Computer Engineering*, Vol. 12, no.2, pp. 69 – 76, 2012.
- [4] Loukriz , M. Haddadi and S. Messalti, "Simulation and experimental design of a new advanced variable step size Incremental Conductance MPPT algorithm for PV systems", *ISA Transactions* , vol.62, pp.30–38, 2016
- [5] Fazia Baghdadi, Kamal Mohammedi, Said Diaf, Omar Behar, "Feasibility study and energy conversion analysis of stand-alone hybrid renewable energy system," *Energy Conversion and Management*, vol. 105, pp. 471–479, 2015
- [6] Aeidapu Mahesh , Kanwarjit Singh Sandhu, "Hybrid wind/photovoltaic energy system developments: Critical review and findings," *Renewable and Sustainable Energy Reviews*, vol. 52, pp. 1135–1147, 2015
- [7] S. Messalti, A. Harrag, A. Loukriz, "A new variable step size neural networks MPPT controller: Review simulation and hardware implementation," *Renewable and Sustainable Energy Reviews*, vol. 68, pp 221–233, 2017
- [8] J. Arfaoui, E. Feki, A. Rabhi, A. Mami. "Optimization of Scaling Factors of Fuzzy–MPPT Controller for Stand-alone Photovoltaic System by Particle Swarm Optimization," 8th International Conference on Sustainability in Energy and Buildings, SEB-16, pp. 11-13 September 2016, Turin, ITALY.
- [9] H. Othmani, D. Mezghani, A. Belaid, A. Mami. "New Approach of Incremental Conductance Algorithm for Maximum Power Point Tracking Based on Fuzzy Logic," *International Journal of Grid and Distributed Computing*, Vol. 9, No. 7, pp. 121-132, 2016
- [10] Unal Yilmaz, Ali Kircay, Selim Borekci. "PV system fuzzy logic MPPT method and PI control as a charge controller," *Renewable and Sustainable Energy Reviews* Vol. 81 pp. 994–1001, 2018
- [11] Manel Jomaa; Mohamed Yassine Allani, Fernando Tadeo, Abdelkader Mami. "Design and control of the hybrid system PV-Wind connected to the DC load," *IEEE International Renewable Energy Congress (IREC)*, Tunisia 2018.
- [12] Joonmin Lee, Young-Seok Kim. "Sensorless fuzzy-logic-based maximum power point tracking control for a small-scale wind power generation systems with a switched mode rectifier," *IET Renew. Power Gener.*, 2016, Vol. 10, pp. 194–202
- [13] Mohamed Akram Jaballah, Dafher Mezghani, Abdelkader Mami. "Design and Simulation of Robust Controllers for Power Electronic Converters used in New Energy Architecture for a (PVG)/ (WTG) Hybrid System," (*IJACSA* International Journal of Advanced Computer Science and Applications, Vol. 8, No. 5, 2017
- [14] Minh-Khai Nguyen, Truong-Duy Duong, Young-Cheol Lim and Yong-Jae Kim, "Isolated Boost DC-DC Converter with Three Switches," *IEEE TRANSACTIONS ON POWER ELECTRONICS*, Vol.33 , pp.1389-1398, Feb. 2018
- [15] Yangjun Lu, Hongfei Wu, Kai Sun, Yan Xing, "A Family of Isolated Buck-Boost Converters Based on Semi-active Rectifiers for High Output Voltage Applications," *IEEE Transactions on Power Electronics*, Vol.31 , pp.6327-6340, Sept. 2016
- [16] V. Indra Gandhi, V. Subramaniaswamy, R. Logesh, "TOPOLOGICAL REVIEW AND ANALYSIS OF DC-DC BOOST CONVERTERS," *Journal of Engineering Science and Technology* Vol. 12, pp.1541-1567, 2017
- [17] Ebrahim Babaei , Zahra Saadatizadeh, "High voltage gain dc-dc converters based on coupled inductors," *IET Power Electronics*, Vol. 11 , pp. 434 – 452 , 3 20 2018
- [18] Bhanu Prashant Reddy Baddipadiga , Venkata Anand Kishore Prabhala, Mehdi Ferdowsi, "A Family of High-Voltage-Gain DC–DC Converters Based on a Generalized Structure," *IEEE Transactions on Power Electronics*, Vol.33 , pp.8399 – 8411, Oct. 2018
- [19] Bhanu Prashanta Reddy Baddipadiga, Mehdi Ferdowsi. "A High-Voltage-Gain DC–DC Converter Based on Modified Dickson Charge Pump Voltage Multiplier," *IEEE Transactions on Power Electronics*, Vol. 32, NO. 10, Octobre 2017.
- [20] Santiago Cóbreces, Robert Griñó, "Hysteretic control of grid-side current for a single-phase LCL grid-connected voltage source converter," *Mathematics and Computers in Simulation*, Vol. 130, pp 194-211, December 2016,
- [21] Fengjiang Wu, Xiaoguang Li, Jiandong Duan, "Improved Elimination Scheme of Current Zero-Crossing Distortion in Unipolar Hysteresis Current Controlled Grid-Connected Inverter," *IEEE Transactions on Industrial Informatics*, Vol. 11 , pp. 1111 - 1118 , Oct. 2015
- [22] Venkata Yaramasu, Bin Wu, "Control of Grid-Side Converters in Wecs," *Wiley-IEEE Press* 2017 Pages: 512
- [23] Sean Cunningham, "THEORY, SIMULATION, AND IMPLEMENTATION OF GRID CONNECTED BACK TO BACK CONVERTERS UTILIZING VOLTAGE ORIENTED CONTROL," May 2017
- [24] Hasan Komurcugil, Necmi Altin, Saban Ozdemir and Ibrahim Sefa, "Lyapunov-Function and Proportional-Resonant Based Control Strategy for Single-Phase Grid-Connected VSI with LCL Filter," *IEEE TRANSACTIONS ON INDUSTRIAL ELECTRONICS*, Vol. 63, pp.2838 – 2849, May 2016
- [25] Abusara, Mohammad A. Sharkh, Suleiman M. Zanchetta, "Pericle Control of grid-connected inverters using adaptive repetitive and proportional resonant schemes," *Journal of Power Electronics*, Vol. 15, pp. 518-529, March 2015
- [26] Mohamed Yassine Allani, Manel Jomaa, Dhafer Mezghani, Abdelkader Mami. "Modelling and Simulation of the hybrid system PV-Wind with MATLAB/SIMULINK," *IEEE International Renewable Energy Congress (IREC)*, Tunisia 2018.
- [27] KHEZZAR, R., ZEREG, M., et KHEZZAR, A. Comparaison entre les différents modèles électriques et détermination des paramètres de la caractéristique IV d'un module

- photovoltaïque. *Revue des énergies renouvelables*, 2010, vol. 13, no 3, p. 379-388.
- [28] Aeidapu Mahesh, Kanwarjit Singh Sandhu, "Hybrid wind/photovoltaic energy system developments: Critical review and findings," *Renewable and Sustainable Energy Reviews*, Vol 52, December 2015, pp. 1135-1147
- [29] Rashid Al Badwawi, Mohammad Abusara, Tapas Mallick. "A Review of Hybrid Solar PV and Wind Energy System," *Smart Science*, Vol. 3, No. 3, pp. 127-138(2015),
- [30] B. Mangu, S. Akshatha, D. Suryanarayana, B.G. Fernandes. "Grid-Connected PV-Win-Battery Based Multi-Input Transformer Coupled Bidirectional DC-DC Converter for Household Applications," *IEEE Journal of Emerging and Selected Topics in Power Electronics*, Vol. 4, NO. 3, Septembre 2016.
- [31] Kivanc Basaran, Numan Sabit Cetin, Selim Borekci. "Energy management for on-grid and off-grid wind/PV and battery hybrid systems," *IET Renew. Power Gener.*, Vol. 11, pp. 642-649, 2017
- [32] Lucas Santana Xavier, Allan F Cupertino, Heverton Augusto.Pereira. "Ancillary services provided by photovoltaic inverters: Single and three phase control strategies," *Computers and Electrical Engineering*, pp. 1–20, 2018
- [33] Majed Althubaiti, Michael Bernard, Petr Musilek. "Fuzzy Logic Controller for Hybrid Renewable Energy System with Multiple Types of Storage," 2017 IEEE 30th Canadian Conference on Electrical and Computer Engineering (CCECE).
- [34] Duy C. Huynh, Matthew W. Dunnigan, "Development and Comparison of an Improved Incremental Conductance Algorithm for Tracking the MPP of a Solar PV Panel," *IEEE Transactions on Sustainable Energy*, Vol. 7, pp. 1421 – 1429, Oct. 2016
- [35] Mohammed Ali Elgendy, David John Atkinson, Bashar Zahawi, "Experimental investigation of the incremental conductance maximum power point tracking algorithm at high perturbation rates", *IET Renewable Power Generation* *IET Renewable Power Generation*, Vol. 10, pp. 133 – 139, 2 2016